# Measurement and understanding of single-molecule break junction rectification caused by asymmetric contacts

Kun Wang, Jianfeng Zhou, Joseph M. Hamill, and Bingqian Xu

Citation: J. Chem. Phys. **141**, 054712 (2014); doi: 10.1063/1.4891862
View online: http://dx.doi.org/10.1063/1.4891862
View Table of Contents: http://aip.scitation.org/toc/jcp/141/5
Published by the American Institute of Physics

# Measurement and understanding of single-molecule break junction rectification caused by asymmetric contacts

Kun Wang, Jianfeng Zhou, Joseph M. Hamill, and Bingqian Xu[a)]
*Single Molecule Study Laboratory, College of Engineering and Nanoscale Science and Engineering Center, University of Georgia, Athens, Georgia 30602, USA*

(Received 17 June 2014; accepted 21 July 2014; published online 7 August 2014)

The contact effects of single-molecule break junctions on rectification behaviors were experimentally explored by a systematic control of anchoring groups of 1,4-disubstituted benzene molecular junctions. Single-molecule conductance and I-V characteristic measurements reveal a strong correlation between rectifying effects and the asymmetry in contacts. Analysis using energy band models and I-V calculations suggested that the rectification behavior is mainly caused by asymmetric coupling strengths at the two contact interfaces. Fitting of the rectification ratio by a modified Simmons model we developed suggests asymmetry in potential drop across the asymmetric anchoring groups as the mechanism of rectifying I-V behavior. This study provides direct experimental evidence and sheds light on the mechanisms of rectification behavior induced simply by contact asymmetry, which serves as an aid to interpret future single-molecule electronic behavior involved with asymmetric contact conformation. © *2014 AIP Publishing LLC*. [http://dx.doi.org/10.1063/1.4891862]

## I. INTRODUCTION

The original considerations of molecular electronics were to search for molecule candidates with rectification behaviors. The experimental attempts of a single-molecule rectifier will pave steps towards future functional molecular electronic devices. Since first proposed by Aviram and Ratner,[1] molecular rectifier has gained considerable attention in both experimental designs[2–5] and theoretical simulations.[6,7] One of the most promising candidates stems from a molecular heterojunction which describes a molecular junction with asymmetric conformation. The asymmetric conformation of a molecular junction was believed to lead to asymmetric electronic behavior such as asymmetric I-V characteristics, a marked feature for future applications as a molecular diode. Within an Au-molecule-Au junction system, the conformational asymmetry could mainly come from two sources: (1) the molecular core and (2) the contacts that bridge the molecule with two electrodes. Compared with steady experimental and theoretical progress on studying molecules with asymmetric molecular core, investigations on the contact effect have not yet come up with a credible response. Although theories predicting the importance of contact interfaces in determining the electron transport properties of molecular wires,[7–10] there have been few experimental attempts to investigate the influences of contact effect on the rectification behavior within a single-molecule break junction. Thus, difficulties exist to draw any conclusion before having thorough understanding of each factor contributing to the final electronic behavior of a molecular junction.

In this paper, we demonstrate a comprehensive investigation on the electronic behavior of molecular junctions with controls on anchoring groups. Using a scanning probe microscopy break junction (SPMBJ) technique,[11] electrical measurements were conducted on molecules with a central benzene ring (B), and alternating anchoring groups of thiol (–SH) and amine ($–NH_2$) in an Au-molecule-Au system. The experimental results indicated a strong correlation between contact circumstance and electronic properties. Rectification behavior was observed when an asymmetric anchoring group was introduced into the junction. Upon theoretical calculations and models, we ascribe the rectification behavior to an asymmetric shift of frontier molecular orbital (FMO) with respect to Fermi levels of the electrodes or an asymmetric potential drop, which essentially roots in the asymmetry of coupling strength at the two contacts. This study provides direct experimental evidence and sheds light on the mechanisms of rectification behavior induced simply by contact asymmetry, which will help to interpret future single-molecule electronic behavior involved with asymmetric contact conformation.

## II. EXPERIMENTAL METHODS

**Choice of sample molecules**: Molecules 1,4-benzenedithiol (SH-B-SH), 1,4-benzenediamine ($NH_2$-B-$NH_2$), and 4-aminothiolphenol (SH-B-$NH_2$) were tested separately in the Au-molecule-Au (Au substrate and Au scanning tunneling microscopy (STM) tip) system upon modified SPM break junction (SPMBJ) technique (Fig. 1(a)). The molecules with benzene ring backbone were chosen because of the smaller energy gap and high degree of $\pi$-conjugation which cause higher electronic transmissions.[12,13] According to Landauer's formalism, the expression of the final transmission efficiency (for simplicity, $T = T_{LC} \times T_{MOL} \times T_{RC}$, where $T_{MOL}$, $T_{LC}$, and $T_{RC}$, respectively, represent transmission efficiencies of molecular core, left contact, and right contact) within a molecular junction incorporates both contact coefficients.[14–16] Therefore, the influence of contacts on electron transport properties of benzene conjugated

a)Author to whom correspondence should be addressed. Electronic mail: bxu@engr.uga.edu. Tel.: +1-706-542-0502.

 

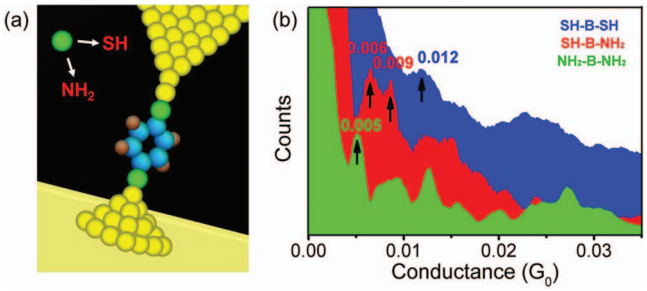


FIG. 1. (a) Schematic of SPMBJ technique: molecules with a central benzene ring (carbon atoms as blue spheres and hydrogen atoms as brown spheres) and alternating anchoring groups (green spheres) of thiol (–SH) and amine ($–NH_2$) in an Au-molecule-Au system. (b) Conductance histograms obtained by wiring SH-B-SH (blue), SH-B-$NH_2$ (red), and $NH_2$-B-$NH_2$ molecules to Au electrodes under 0.3 V, respectively. The counts value for each histogram is shifted vertically to show the relative position of conductance peaks for different molecules.

molecular junctions could be more pronounced since the simple and symmetric central molecular backbone excludes most distortions from molecular structure itself. Thus, the change of electronic properties primarily roots in the contact parts. These features make 1,4-disubstituted benzene molecules one of the best candidates for contact effect study.

**Chemicals and sample preparation**: 1,4-benzenediamine (purity, 97%) and 4-aminothiolphenol (purity, 97%) were purchased from Aldrich. 1,4-benzenedithiol (purity, 97%) was purchased from Alfa Aesar. For Au substrate deposition, the gold beads come from Kurt J. Lesker company (99.999%), and mica sheets (Grade V1) were from Ted Pella, Inc. Au substrates were prepared by evaporating ~100 nm of gold onto freshly cleaved mica sheets using thermal evaporation in a vacuum of $10^{-7}$ Torr. The surfaces of Au substrates were annealed by hydrogen flame just before immersion in sample solutions. This annealing step cleaned the surface and allowed epitaxial reconstruction of the Au to form large terraces of Au (111). All molecules were prepared as 1 mM solutions in toluene. Each sample solution was put into a liquid cell and a self-assembled monolayer (SAM) was formed on an Au substrate after 6 h exposure. Then the coated samples were fixed in the STM system for the characterization. A 0.25 mm diameter gold wire (purity, 99.999%, Alfa Aesar) was sharply cut and then coated with wax as STM tips before each experiment. A STM scanner with 1000 nA/V preamplifier was applied for all measurements.

**Single-molecule conductance and I-V characteristic measurements:** The measurements of single-molecule conductance were performed using a SPMBJ technique. Under a constant 0.3 V bias, the STM tip was driven by piezoelectric transducer (PZT) continuously towards and away from Au substrate to form and break molecular junctions. Conductance traces were repeatedly recorded during the retracting process where the STM tip was pulled away from Au substrate. For each measurement, around 1000 traces were collected for the construction of a conductance histogram. In the final conductance histogram, the most prominent peak was the most probable conductance of corresponding molecular junction. In addition, I-V curves of each molecular junction were measured using a modified SPMBJ technique,[17] where the tip retracting process was divided into multiple periodic processes each of which contained two parts: abrupt stretching and free holding. Using a homemade Labview program, with the constant 0.3 V nulled by a reverse bias, an I-V sweep from –1 V to 1 V was applied on each free holding process. Thus I-V curves of single molecular junction could be collected whenever one molecule was wired between the tip and substrate. In all experiments, the bias was consistently applied on the Au substrate with the STM tip grounded. In total two groups of molecular junctions employing different molecules were characterized: (i) symmetric molecular junctions, Au-SH-B-SH-Au and Au-$NH_2$-B-$NH_2$-Au; (ii) molecular junctions with asymmetric anchoring groups, Au-SH-B-$NH_2$-Au or Au-$NH_2$-B-SH-Au. Here, the molecular junction was represented in the form of substrate-molecule-tip and this applies to all junctions subsequently referred to in this paper.

## III. RESULTS AND DISCUSSION

### A. Single-molecule conductance measurements

We carried out the single-molecule conductance measurements by separately wiring three molecules in the Au-molecule-Au junction system and creating conductance histograms from the resulting data (see Fig. 1(b)). Noticeably, the Au-$NH_2$-B-$NH_2$-Au conductance histogram (green, 726 in ~1300 traces) shows thin but pronounced peaks. The value of the first peak (0.005 $G_0$) is close to other previously reported values.[18,19] In the histogram of Au-SH-B-SH-Au (blue, 806 in ~1300 traces), a set of dominant conductance peaks is identified. The conductance value was 0.012 $G_0$ also coinciding with reported values.[20] Interestingly, compared with Au-$NH_2$-B-$NH_2$-Au, the conductance value of the Au-SH-B-SH-Au is much higher and the distributions of conductance peaks become broader although they have identical electrodes and the central molecular core. This shape difference of the histograms is therefore attributed to the different anchoring groups. It was reported that the local amine-Au bonding geometry is remarkably well-defined, with the amine group only binding to undercoordinated Au sites.[19] While, as justified in other discussions,[21,22] the stronger but more flexible Au–SH bonds may bring perturbations into the junction and consequently result in a wide distribution in molecular conductance. In contrast with the above two molecules, the conductance histogram (red, 711 in ~1300 traces) reveals two separate single-molecule conductance peak values (0.006 $G_0$ and 0.009 $G_0$) when SH-B-$NH_2$ was wired to the system. Both conductance values are located between those of Au-$NH_2$-B-$NH_2$-Au and Au-SH-B-SH-Au. We believe this is due to the relatively stronger Au–SH bond within the junction that breaks the symmetry and produces two junction conformations with –SH bonding to either the Au substrate or Au tip. The formation of two separate conductance peaks should be attributed to asymmetric electronic properties of the two molecular junctions.

### B. I-V characteristics for different molecular junctions

To further probe the influences of asymmetric contacts under a bias sweep (−1 V to 1 V), single molecular I-V characteristics were measured for all molecules. Typical

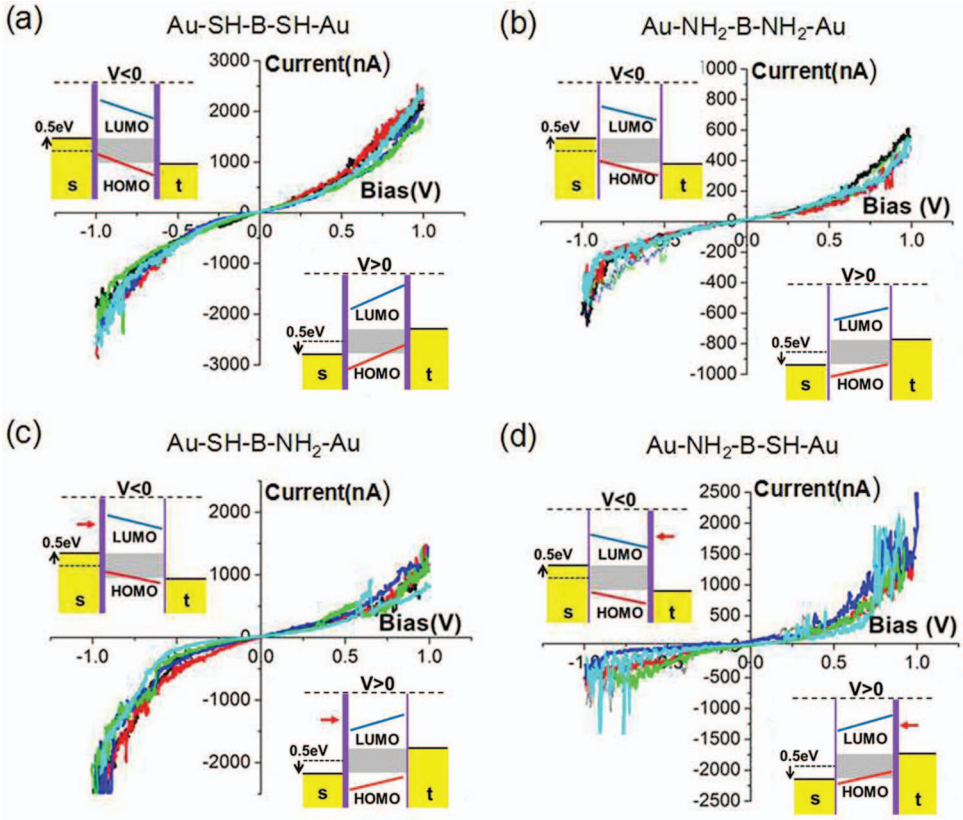


FIG. 2. (a)–(d) The I-V characteristics (5 representative curves for each) and the corresponding energy band diagrams for each molecular junction. The red arrows in the energy band diagrams point at the contact with a relatively stronger coupling strength.

I-V curves for each molecular junction are plotted in Fig. 2. For symmetric molecular junctions Au-SH-B-SH-Au and Au-$NH_2$-B-$NH_2$-Au, their I-V curves are also symmetric (Figs. 2(a) and 2(b)). But molecular junction Au-SH-B-SH-Au produced much higher current (∼2500 nA) at +1/−1 V than Au-$NH_2$-B-$NH_2$-Au (∼700 nA) does. This is in accordance with the conductance measurement results at 0.3 V. In sharp contrast, when molecule SH-B-$NH_2$ is bridged between Au electrodes, the I-V curves reveal pronounced rectification behavior. Interestingly, the rectified I-V curves illustrate higher current under either negative bias or positive bias despite that only one type of molecule was in the junction. This implies that the molecular junction alternates between two possible conformations on the basis of whether –SH anchoring group is wired to either Au tip or Au substrate. Thus at 0.3 V, two different current values can both be observed. This explains the fact that two single-molecule conductance sets were observed in the conductance histograms (Fig. 1(b), red). Noticeably, for rectified I-V curves, the higher current goes up to ∼2500 nA which is similar to the ending current of Au-SH-B-SH-Au and the lower current ends at ∼1000 nA which is similar to that of Au-$NH_2$-B-SH-Au, suggesting that SH-B-$NH_2$ bridged between Au electrodes is a hybrid system of Au-SH-B-SH-Au and Au-$NH_2$-B-$NH_2$-Au molecular junctions.

### C. Differential conductance (dI/dV)

To understand the I-V characteristics, differential conductance (dI/dV) profiles are constructed to illustrate the local density of states (LDOS) change introduced with different contact conformation (Fig. 3). The dI/dV curves were calculated using the smoothed I-V curves of the raw I-V curves shown in Fig. 2. The smoothing greatly reduced the fluctuation on the I-V curves but still maintained the global trend of the rectifying effect. This could avoid most of the insignificant information caused by those fluctuations in dI/dV plots. The peaks in a dI/dV plot have been suggested to imply extra conduction states.[23] In agreement with I-V characteristics, the

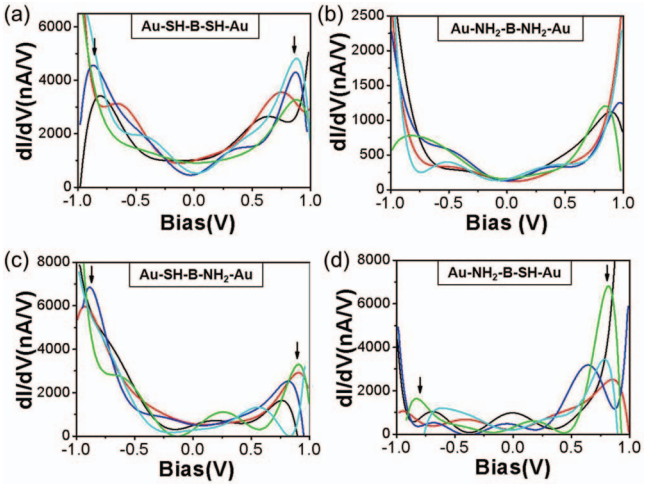


FIG. 3. (a)–(d) Differential conductance (dI/dV) profiles for each molecular junction. The arrows in the profiles represent the peak position observed from the dI/dV profiles.

dI/dV plots reveal symmetric profiles for symmetric junctions Au-SH-B-SH-Au and Au-$NH_2$-B-$NH_2$-Au. The symmetry in peak height and position in dI/dV profile of Au-SH-B-SH-Au also indicate a similar LDOS increase under both positive and negative bias. There is no obvious peak in the dI/dV profiles of Au-$NH_2$-B-$NH_2$-Au, indicating trivial changes in LDOS within the applied bias range. However, for Au-SH-B-$NH_2$-Au and Au-$NH_2$-B-SH-Au, pronounced asymmetry in peak height under different bias polarities is observed although the peak position is nearly symmetric. According to dI/dV profiles, much more LDOS are activated under the bias regime where higher current takes place than the lower current side. Interestingly, the asymmetry of LDOS starts at around 0.4 V for I-V curves with higher current at negative bias, which is much earlier than those (0.6 V) with higher current under positive bias. It has to be noted that the inevitable peaks induced by the noise on I-V curves may still exist in dI/dV plot for those rough I-V curves even after smoothing. But the most peaks in dI/dV should be related to the increase in conduction states.

### D. Energy band model

To gain insights into the mechanisms causing molecular rectification behavior, multiple theoretical mechanisms have been developed, such as the models of Williams,[24] Baranger,[25] Ford,[26] and Whitesides *et al.*[27] In an asymmetric contact system like ours, the decisive factor rests with the coupling strength between the terminal of the molecules and the electrodes. When an asymmetric component is introduced, the coupling strength at either contact is also asymmetric. As an analogy to the two-barrier model commonly used in the rectification study of asymmetric molecules,[26] the contact with a stronger coupling between the molecule and electrode resembles a narrower barrier through which electrons tunnel across more easily. Oppositely, the contact with a weaker coupling performs like a broader barrier requiring higher energy to access the electron transport. Based on a model recently proposed by Zhao *et al.*,[28] stronger coupling signifies a closer affinity between the FMO and Fermi levels of the electrodes. In this model, the FMO tends to shift with the Fermi level of the strongly coupled electrode as a whole, when a bias is applied. Thus, at the strongly coupled contact, the absolute difference between FMO of the molecule and Fermi level of the electrode nearly remains constant during the shift. However, at the weaker contact, the FMO shifts independently creating a lag with the movement of Fermi level of the electrode, which either increases or decreases the difference between FMO and Fermi level of the electrode under zero bias. Then, for the weak contact, this difference will increase whenever Fermi level of the electrode shifts up and it decreases whenever Fermi level of the electrode shifts down. The dominating FMO has been proven to be HOMO orbital for molecules used in our experiments.[19,29] It has to be noted that LUMO orbitals are far out of the bias window in our experiments on account of the HOMO-LUMO gap (4–5 eV) for these molecules.

To explain the experimental results, coupling strength introduced with various contact conformations needs to be clarified. Binding energies of contact bonds in our study have been calculated to be 0.37 eV for Au–$NH_2$ and 1.60 eV for Au–SH.[18,29,30] It is believed that a higher binding energy implies a stronger coupling between the molecule and the electrode,[18,29] indicating a much stronger coupling for Au–SH than for Au–$NH_2$. Theoretical calculations[10,19] suggested that factors like the local bonding length and junction elongation and tilt would not be the major effect within our bias window, which rules out the concerns on the related influence caused by these factors.

We plot the energy band diagram for each molecular junction as the inset in Fig. 2. For Au-SH-B-SH-Au and Au-$NH_2$-B-$NH_2$-Au junctions, the coupling strength at both contacts was identical. As Fermi levels of the electrodes shift under a bias sweep, the relative difference between MOs and electrodes remains nearly constant at either contact. Hence, similar delocalized states would be obtained under both bias polarities. Namely, a symmetric I-V characteristic should be observed, which agrees with experimental I-V curves (Figs. 2(a) and 2(b)). For junctions with asymmetric anchoring groups like Au-SH-B-$NH_2$-Au or Au-$NH_2$-B-SH-Au, the coupling strength of Au-SH is much stronger than that of Au-$NH_2$, delocalizing more states when the Fermi level of the strongly coupled electrode shifts up. Therefore, for the Au-SH-B-$NH_2$-Au junction where –SH is wired to Au substrate, higher current should be obtained under negative bias as illustrated in experimental I-V curves (Fig. 2(c)). Oppositely, I-V characteristic for the other orientation Au-$NH_2$-B-SH-Au reveals a reversed rectification with higher current at positive bias which was also in accordance with this model.

### E. I-V calculations

#### 1. Transition voltage spectroscopy (TVS)

A Fowler-Nordheim (F-N) plot of an I-V curve measured from a SMBJ can yield minima at specific transition voltages.[31] The bias voltage at a specific minimum signifies the transition voltage where a trapezoid shaped tunneling barrier turns to a triangle shaped barrier. It is important to note that the transition voltage is usually smaller than the bias potential necessary for the resonant tunneling. As is shown in Fig. 4, for symmetric junctions Au-SH-B-SH-Au and

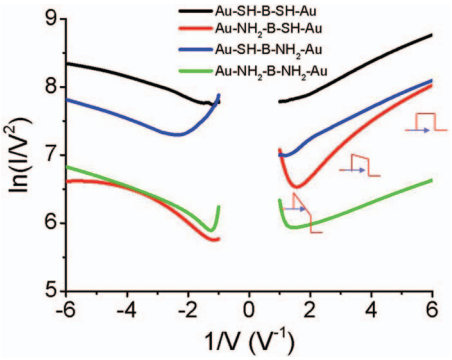


FIG. 4. F-N plots for each molecular junction. The change in tunneling barrier from rectangular shape, trapezoid shape to triangle shape is demonstrated along the F-N curve of Au-$NH_2$-B-SH-Au (red).

Au-$NH_2$-B-$NH_2$-Au, relatively symmetric features were observed in the F-N curves (black and green). But the F-N curve of Au-SH-B-SH-Au lacks the well-defined minima which were observed in the F-N curve of Au-$NH_2$-B-$NH_2$-Au. This suggests that the transition voltage for Au-SH-B-SH-Au lies outside the bias window (−1 to 1 V) applied in our experiments. For the two asymmetric junctions, only one side of F-N plots show pronounced minimum and the displacement of F-N curves is rather asymmetric. The transition voltages for Au-SH-B-$NH_2$-Au and Au-$NH_2$-B-SH-Au are determined to be −0.45 V and 0.65 V, respectively. The transition voltages for Au-$NH_2$-B-$NH_2$-Au are determined to be −0.85 V and 0.85 V under negative and positive bias, respectively. Previous study suggested that a relatively weak binding energy leads to a smaller difference between the Fermi level of electrodes and FMO.[29] This may explain why transition voltage of Au-$NH_2$-B-$NH_2$-Au is reached earlier than that of Au-SH-B-SH-Au. Using the well-defined minima at both sides of the F-N plot for Au-$NH_2$-B-$NH_2$-Au, the energy gap $\varepsilon$ between the Fermi level of the electrodes and FMO is calculated to be 0.69 eV, suggesting that the HOMO of $NH_2$-B-$NH_2$ is still outside the conduction window (−0.5 eV to 0.5 eV). Due to the lack of well-defined minima at both sides of the F-N curves for the other molecular junctions, it is not possible to derive the energy gap via transition voltage spectroscopy (TVS) analysis.

### 2. Landauer Fitting

An I-V curve can also be fit to a simplified Landauer formula, Eq. (1), using a Levenberg-Marquardt least squares fitting algorithm:[32]

$$I(V) \propto \int_{-\infty}^{\infty} T(E,V)\left[f\left(E-\frac{eV}{2}\right)-f\left(E+\frac{eV}{2}\right)\right]dE, \tag{1}$$

where

$$T(E,V) = 4\Gamma_L\Gamma_R\left\{\left[E-\varepsilon-\frac{eV}{2}\left(\frac{\Gamma_L-\Gamma_R}{\Gamma_L+\Gamma_R}\right)\right]^2+[\Gamma_L+\Gamma_R]^2\right\}^{-1}. \tag{2}$$

Using Eqs. (1) and (2), experimental I-V curves can be fitted to three parameters.[33] The three parameters correspond to the gap $\varepsilon$, and the degree of coupling, $\Gamma_L$ and $\Gamma_R$, to each electrode separately. When this fitting method was applied to the different junctions with variable anchoring groups, the results agreed with observations made from the qualitative analysis of the I-V curves (see Table I). The junctions when symmetric yielded symmetric values for $\Gamma_L$ and $\Gamma_R$, and yield unequal values when the junctions were asymmetric. This provides a quantitative confirmation for the observation that the asymmetric junctions yielded asymmetric I-V curves due to unequal coupling to the molecule.

The energy gap for Au-$NH_2$-B-$NH_2$-Au calculated from Landauer fitting is close to the results of TVS analysis. And two symmetric junctions yield a similar energy gap value, which is close to previous reported value.[19] We see that the $\Gamma$ value for Au–SH is larger than Au–$NH_2$, which coincides with the previous bonding energy calculations. We also find the introduction of asymmetric anchoring groups alters the FMO and increases the energy gap in asymmetric junctions. It is apparent the energy gap for all molecular junctions is over the applied external energy (0.5 eV) applied in our experiments. Overall, the Landauer fitting results imply a non-resonant tunnelling charge transport for all molecular junctions and asymmetric coupling strength at the molecule-electrode contact as the cause of the rectification behaviour.

TABLE I. Landauer formula fitting results for all molecular junctions.

| Molecular junction | $\Gamma_L$ (eV) | $\Gamma_R$ (eV) | $\varepsilon_{fit}$ (eV) |
|---|---|---|---|
| Au-$NH_2$-B-$NH_2$-Au | $1.49 \times 10^{-2}$ | $1.52 \times 10^{-2}$ | 0.636 |
| Au-SH-B-SH-Au | $3.95 \times 10^{-2}$ | $3.86 \times 10^{-2}$ | 0.698 |
| Au-SH-B-$NH_2$-Au | $6.32 \times 10^{-2}$ | $2.92 \times 10^{-2}$ | 0.848 |
| Au-$NH_2$-B-SH-Au | $1.77 \times 10^{-2}$ | $2.71 \times 10^{-2}$ | 0.735 |

### F. Rectification ratio model

The rectification ratio (RR) calculation reflects the degree of asymmetry as a function of applied bias for asymmetric I-V characteristics. Here we define RR = $|I_{high}/I_{low}|$. RR for all molecular junctions is plotted in Fig. 5 and Ref. 30. As expected, the RR for symmetric junctions stays around 1 across the whole bias range, indicating a nearly equal current under positive and negative bias. We see the RR for Au-SH-B-$NH_2$-Au stays around 1 at lower bias range (0–0.3 V), starts increasing at around 0.4 V, and ends over 5 at 1 V. RR for Au-$NH_2$-B-SH-Au starts increasing later at around 0.6 V and ends around 3 at 1 V. The onset voltages of rectification, where RR starts increasing beyond 1, agree well with the transition voltages determined by TVS analysis. We ascribe the difference

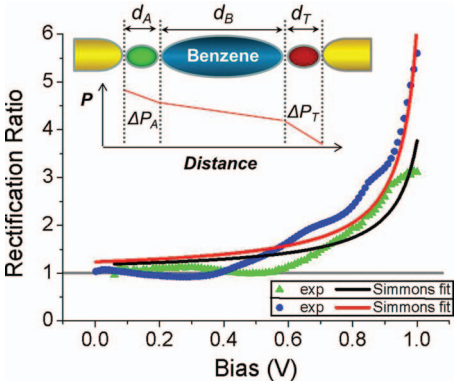


FIG. 5. Rectification ratio plot for asymmetric junctions of experimental data and corresponding fitting using Eq. (6): Au-$NH_2$-B-SH-Au (green triangle for experimental data and black curve for Simmons fit) and Au-SH-B-$NH_2$-Au (blue circle for experimental data and red curve for Simmons fit). The inset shows a schematic of potential drop across different segments of the molecular junctions. $d_B$ is the length of the benzene molecular core and $d_A$ and $d_T$ represent the length of amine and thiol anchoring groups, respectively. $\Delta P_A$ and $\Delta P_T$ represent the potential drop along amine group and thiol group, respectively. The modified Simmons model only cares about the change in potential drop difference $\Delta P = |\Delta P_A - \Delta P_T|$ from forward bias regime to reverse bias regime.

in onset voltage for two asymmetric junctions to different contact geometries induced via bonding thiol group to the sharp Au tip or the flat Au substrate.

Using the Simmons model[34,35] with image potential included, the current density for intermediate voltage range applicable for our experiment is given by

$$J = J_0[\varphi \exp(-\kappa\beta_m\sqrt{\varphi}) - (\varphi + eV) \times \exp(-\kappa\beta_m\sqrt{\varphi + eV})], \quad (3)$$

where

$$J_0 = \frac{e}{2\pi h(\beta_m d)^2}$$

and

$$\kappa = \frac{4\pi d\sqrt{2m_e^*}}{h},$$

where $\varphi$ is the average value of the barrier height considering image potential, $\beta_m$ is the barrier decay constant, $d$ is the distance across the barrier along the whole molecular junction including end groups, $h$ is Plank constant, and $m_e^*$ is the effective mass of electron. Noticeably, the barrier width is not considered since it is not parameterized in Simmons model. A non-unity rectification can be explained by an asymmetric potential drop across the end group-molecule-end group system when the end groups are not identical as the inset schematic of Fig. 5 shows. Here we assume that the potential drop across the benzene molecular core is always the same under forward bias and reverse bias. Defining forward bias to refer to the half of the I-V curve which has higher current, and reverse bias to refer to the lower current half, we can account for this difference in current as a stronger potential drop ($\Delta P = |\Delta P_A - \Delta P_T|$) in the reverse bias direction across the end group which dominates the electron transport over the other end group, and a negligible potential drop across the same end group during the forward bias direction.[36] This case can be incorporated into the Simmons formula by adding a term to account for the influence of the extra barrier decay ($\Delta\beta$) for the end group during the reverse bias. Thus, the current density under forward bias and reverse bias can be written as

$$J_{forward} = \frac{\lambda}{\beta_m^2}[\varphi \exp(-\kappa\beta_m\sqrt{\varphi}) - (\varphi + eV)\exp(-\kappa\beta_m\sqrt{\varphi + eV})], \quad (4)$$

$$J_{reverse} = \frac{\lambda}{(\beta_m + \Delta\beta)^2}[\varphi \exp(-\kappa(\beta_m + \Delta\beta)\sqrt{\varphi}) - (\varphi + eV)\exp(-\kappa(\beta_m + \Delta\beta)\sqrt{\varphi + eV})], \quad (5)$$

where $\lambda = \frac{e}{2\pi hd^2}$.

Using these two forms (Eqs. (4) and (5)) of the Simmons formula, a formula for the rectification ratio of asymmetric junctions can be derived as

$$RR(V) = \frac{J_{forward}}{J_{reverse}} = \frac{B^2}{A^2} \times \frac{\varphi \exp\left(-A\sqrt{\varphi}\right) - (\varphi + eV)\exp\left(-A\sqrt{\varphi + eV}\right)}{\varphi \exp\left(-B\sqrt{\varphi}\right) - (\varphi + eV)\exp\left(-B\sqrt{\varphi + eV}\right)}, \quad (6)$$

where

$$A = \kappa\beta_m$$

and

$$B = \kappa(\beta_m + \Delta\beta).$$

TABLE II. The modified Simmons model fitting parameters for two asymmetric junctions.

| Molecular junction | $A$ | $B$ | $\Phi$ (eV) | $\Delta\beta/\beta_m$ |
|---|---|---|---|---|
| Au-$NH_2$-B-SH-Au | 1.673 | 1.712 | 1.893 | 3.9% |
| Au-SH-B-$NH_2$-Au | 2.993 | 3.149 | 1.704 | 5.0% |

Fitting our experimental RR curves to Eq. (6) yields essential information about the junction. Equation (6) leaves only three fitting parameters: $A$, $B$, and $\varphi$. The fitting curves for asymmetric junctions are also illustrated in Fig. 5. First, notice that the rectification ratio for the Au-$NH_2$-B-SH-Au junction was calculated using I(+V)/I(−V), while for Au-SH-B-$NH_2$-Au the inverse was used based on our definition. This approach assured us that the rectification ratio was >1 for most of the curve. Fitting parameters are shown in Table II.

For both junctions, the fitting parameters indicate that an extra decay constant or larger potential drop occurs under the reverse bias regime, introducing the asymmetry in potential drop and creating the rectification. But Au-$NH_2$-B-SH-Au has a slightly higher barrier than Au-SH-B-$NH_2$-Au does. The $\Delta\beta/\beta_m$ value reveals the proportion of additional decay constant added to the forward bias decay constant when under the reverse bias. Au-SH-B-$NH_2$-Au has a greater $\Delta\beta/\beta_m$ (5.0%), suggesting a larger relative potential drop occurring in the reverse bias regime than that (3.9%) for Au-$NH_2$-B-$NH_2$-Au. This also implies a higher RR for Au-SH-B-$NH_2$-Au, as we observed from the experimental data (blue circle in Fig. 5). Similar fitting yields a straight line with a value of around 1 for both symmetric junctions,[33] which suggests a symmetric potential drop under both bias polarities. This is also in accordance with experimental I-V curves.

The Simmons approximation to the Landauer's formula has proven to be a very powerful tool to study molecular break junctions. However, its canonical form Eq. (3) is unable to accommodate asymmetric junctions because it was explicitly derived for symmetric junctions.[34] By rewriting the Simmons formula in the form of a rectification ratio, asymmetry can be explicitly incorporated into the formula. This provides a physical model to describe the rectification behaviour of any single molecular I-V curve, and adapts the Simmons model for broader use than its original application. Furthermore, it provides a tool to explicitly calculate the contribution of the end groups to the overall character of the I-V curve.

The theoretical analysis demonstrated above provides multiple ways to understand the physical meaning of obtained experimental data. In our study, the rectification behaviour of a molecular junction with different anchoring groups is suggested to be induced by an asymmetric relative shift of FMO with respect to Fermi level of the electrode in the energy band model, an asymmetric displacement of transition voltages in TVS analysis, an asymmetric coupling degree in Landauer fitting and asymmetric potential drop in the modified Simmons model. Significant information like this offers us the chance to thoroughly understand the nature of charge transport property within a molecular junction and paves steps towards the ultimate molecular devices. Noticeably, by isolating the contact part, we have studied the rectification behaviour simply induced by the asymmetry in contact coupling, which is different from the donor-acceptor model developed for asymmetric molecular core.[37,38] Interestingly, the rectification ratio we obtained is comparable to some of the donor-acceptor molecules,[27] which again highlights the influence of the contact interfaces.

## IV. CONCLUSIONS

In summary, by experimentally exploring the electron transport properties of molecular junctions with asymmetric contact conformations, we have demonstrated a systematic investigation of molecular rectification behavior regarding contact effect of asymmetric anchoring group. Rectification behavior was observed under asymmetric contact conditions. Using theoretical models and calculations, the cause of rectification behavior is mainly attributed to asymmetric coupling strength at the two contacts which leads to an asymmetric relative shift between FMO and Fermi level of the electrodes. A newly modified Simmons model allows us to extract critical parameters from the experimental rectification ratio curve. Using this model, we find that the rectification can also be ascribed to asymmetric potential drop under forward bias and reverse bias. Our results provide important information in understanding the mechanisms of rectification behaviors. Overall, our study will give opportunity to complete the picture of electronic properties related to rectification behaviors in various molecular junctions with asymmetric contacts.

## ACKNOWLEDGMENTS

The authors thank the U.S. National Science Foundation for funding this work (Grant Nos. ECCS 0823849 and ECCS 1231967).

[1]A. Aviram and M. A. Ratner, Chem. Phys. Lett. **29**, 277 (1974).
[2]A. Batra, P. Darancet, Q. Chen, J. S. Meisner, J. R. Widawsky, J. B. Neaton, C. Nuckolls, and L. Venkataraman, Nano Lett. **13**, 6233 (2013).
[3]S. K. Yee, J. Sun, P. Darancet, T. D. Tilley, A. Majumdar, J. B. Neaton, and R. A. Segalman, ACS Nano **5**, 9256 (2011).
[4]E. Loertscher, B. Gotsmann, Y. Lee, L. Yu, C. Rettner, and H. Riel, ACS Nano **6**, 4931 (2012).
[5]X. Chen, S. Yeganeh, L. Qin, S. Li, C. Xue, A. B. Braunschweig, G. C. Schatz, M. A. Ratner, and C. A. Mirkin, Nano Lett. **9**, 3974 (2009).
[6]C. Toher, I. Rungger, and S. Sanvito, Phys. Rev. B **79**, 205427 (2009).
[7]G.-P. Zhang, G.-C. Hu, Y. Song, Z.-L. Li, and C.-K. Wang, J. Phys. Chem. C **116**, 22009 (2012).
[8]Y. Lee, B. Carsten, and L. Yu, Langmuir **25**, 1495 (2009).
[9]M. Kiguchi, H. Nakamura, Y. Takahashi, T. Takahashi, and T. Ohto, J. Phys. Chem. C **114**, 22254 (2010).
[10]K. B. Dhungana, S. Mandal, and R. Pati, J. Phys. Chem. C **116**, 17268 (2012).
[11]B. Q. Xu and N. J. J. Tao, Science **301**, 1221 (2003).
[12]Y. Q. Xue and M. A. Ratner, Phys. Rev. B **68**, 115406 (2003).
[13]H. Song, Y. Kim, Y. H. Jang, H. Jeong, M. A. Reed, and T. Lee, Nature (London) **462**, 1039 (2009).
[14]A. Salomon, D. Cahen, S. Lindsay, J. Tomfohr, V. B. Engelkes, and C. D. Frisbie, Adv. Mater. **15**, 1881 (2003).
[15]J. Zhou, C. Guo, and B. Xu, J. Phys.: Condens. Matter **24**, 164209 (2012).
[16]H. B. Akkerman and B. de Boer, J. Phys.: Condens. Matter **20**, 013001 (2008).
[17]J. Zhou, F. Chen, and B. Xu, J. Am. Chem. Soc. **131**, 10439 (2009).
[18]M. Tsutsui, M. Taniguchi, and T. Kawai, J. Am. Chem. Soc. **131**, 10552 (2009).
[19]S. Y. Quek, L. Venkataraman, H. J. Choi, S. G. Louie, M. S. Hybertsen, and J. B. Neaton, Nano Lett. **7**, 3477 (2007).
[20]X. Y. Xiao, B. Q. Xu, and N. J. Tao, Nano Lett. **4**, 267 (2004).
[21]L. Venkataraman, J. E. Klare, I. W. Tam, C. Nuckolls, M. S. Hybertsen, and M. L. Steigerwald, Nano Lett. **6**, 458 (2006).
[22]J. Zhou, G. Chen, and B. Xu, J. Phys. Chem. C **114**, 8587 (2010).
[23]J. Hihath, C. Bruot, H. Nakamura, Y. Asai, I. Diez-Perez, Y. Lee, L. Yu, and N. Tao, ACS Nano **5**, 8331 (2011).
[24]P. E. Kornilovitch, A. M. Bratkovsky, and R. S. Williams, Phys. Rev. B **66**, 165436 (2002).
[25]R. Liu, S. H. Ke, W. T. Yang, and H. U. Baranger, J. Chem. Phys. **124**, 024718 (2006).
[26]N. Armstrong, R. C. Hoft, A. McDonagh, M. B. Cortie, and M. J. Ford, Nano Lett. **7**, 3018 (2007).
[27]C. A. Nijhuis, W. F. Reus, and G. M. Whitesides, J. Am. Chem. Soc. **132**, 18386 (2010).
[28]J. Zhao, C. Yu, N. Wang, and H. Liu, J. Phys. Chem. C **114**, 4135 (2010).
[29]M. Kiguchi, S. Miura, T. Takahashi, K. Hara, M. Sawamura, and K. Murakoshi, J. Phys. Chem. C **112**, 13349 (2008).
[30]S. Miranda-Rojas, A. Munoz-Castro, R. Arratia-Perez, and F. Mendizabal, Phys. Chem. Chem. Phys. **15**, 20363 (2013).
[31]J. M. Beebe, B. Kim, J. W. Gadzuk, C. D. Frisbie, and J. G. Kushmerick, Phys. Rev. Lett. **97**, 026801 (2006).
[32]B. M. Briechle, Y. Kim, P. Ehrenreich, A. Erbe, D. Sysoiev, T. Huhn, U. Groth, and E. Scheer, Beilstein J. Nanotech. **3**, 798 (2012).
[33]See supplementary material at http://dx.doi.org/10.1063/1.4891862 for Landauer fitting curves and the modified Simmons model fitting of symmetric junctions Au-SH-B-SH-Au and Au-NH2-B-NH2-Au.
[34]J. G. Simmons, J. Appl. Phys. **34**, 1793 (1963).
[35]H. B. Akkerman, R. C. G. Naber, B. Jongbloed, P. A. van Hal, P. W. M. Blom, D. M. de Leeuw, and B. de Boer, Proc. Natl. Acad. Sci. U.S.A. **104**, 11161 (2007).
[36]B. Cui, Y. Xu, G. Ji, H. Wang, W. Zhao, Y. Zhai, D. Li, and D. Liu, Org. Electron. **15**, 484 (2014).
[37]G. J. Ashwell, W. D. Tyrrell, and A. J. Whittam, J. Am. Chem. Soc. **126**, 7102 (2004).
[38]G. J. Ashwell, B. Urasinska, and W. D. Tyrrell, Phys. Chem. Chem. Phys. **8**, 3314 (2006).